Optimal Transport: an application to the RADAR Recognition Process for deinterleaving RADAR pulses and identifying emitters

Manon Mottier [1,2]

Supervised by Gilles Chardon [2], Frédéric Pascal [2]
Chakib Belafdil [1] & Jean-Daniel Busi [1]

[1] *Avantix, Aix-en-Provence, France*
[2] *The Signals and System Laboratory (L2S) from CentraleSupélec at Paris-Saclay University*

Supervision & funding

- **Industrial thesis**: Artificial Intelligence for Passive RADAR
  - The Signals and System Laboratory (L2S) from CentraleSupélec at Paris-Saclay University
    - → Co-supervisor: Gilles Chardon
    - → Thesis director: Frédéric Pascal
  - Avantix, a French company specialized in Electronic Warfare:
    - → Co-supervisor: Chakib Belafdil
    - → Supervisor: Jean-Daniel Busi

CentraleSupélec

université PARIS-SACLAY

L2S Laboratoire Signaux & Systèmes

AVANTIX

Content

The challenges of RADAR signal processing

- Avantix designs critical high-tech systems to provide homeland protection and military forces.
- Provides strategic information to military platforms:
  - → Identifying the enemies gives a considerable advantage (decision-making, commitment ...),
  - → Anticipating the actions and setting up adapted measures.
- Use and development of machine learning tools for **passive RADAR**.
- Improving the **RADAR Recognition Process** [1, 2] with **Optimal Transport** theory [3, 4, 5]:
  1. Deinterleaving RADAR pulses from a signal,
  2. Identification of RADAR from a set of pulses.

RAdio Detection And Ranging

What is a passive RADAR?

- Emit no electromagnetic waves
- Only receivers
- Detect, track, and identify other emitters(s)
  - → Monitoring discreetly
  - → Minimizing interference or disruption
  - → Cost optimization

➠ Focus on identification for ELINT [1, 6, 7]

Figure: ELINT RESM.

RADAR Recognition Process

1 Deinterleaving RADAR pulses from a signal

- **Definition:** Separating and grouping the mixed pulses coming from an unknown number of emitters in a signal.
- ? **Existing methods:**
  - → Pulse repetition intervals, frequency, direction of arrival [8, 9, 6],
  - → Clustering [10, 11, 12],
  - → Deep Learning [13, 14, 15],
  - → ...
- ✘ **Limitations:** Supervised methods, only efficient on simple RADAR, need a lot of data...
- **Our solution:** Pulses separation with HDBSCAN and cluster fusion with Hierarchical Agglomerative Clustering using Optimal Transport Distances.

RADAR Recognition Process

❷ Identification of RADAR from a set of pulses

☛ **Definition:** Feature extraction and comparison with a reference database to identify the RADAR present in a signal.

? **Existing methods:**

→ Time-frequency analysis [16, 17],

→ Deep learning [18, 19, 20],

→ ...

✘ **Limitations:** Supervised methods, few classes, model retrained, performance depends on simulator accuracy, lots of settings ...

☛ **Our solution:** Developing a distance between a set of pulses and emitter classes using the Optimal Transport Distances and the missing pulses rate modelization for the Pulse Repetition of Intervals.

Content

Methodology

- Methods developed from a simulator and validated on real data:
  - Simulator developed by our knowledge of the radar environment,
  - Receptor static, omnidirectional, and has known detection threshold,
  - No consideration of adverse measures introducing disruptive signals.
- 2 steps for signal simulation:
  1. Creation of a database gathering the emitters' characteristics,
  2. Simulation of a signal from these characteristics according to the parameters set by the user (noise, number of emitters in the signal, size...).

Emitters class database

Emitter described by:

- **Technical emitter parameters**: Power Transmitted (Pow_t), transmit antenna gain (Gn_t), scan period (S), or antenna length (y).
- **Pulses parameters**: Frequency (F, f_n), pulse width (PW, pw_n), level (G, g_n), or pulse repetition interval pattern (PRI, pri_n).

Emitters characteristics example

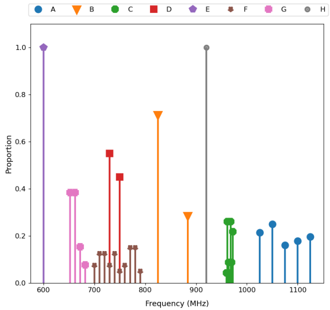

Frequency.

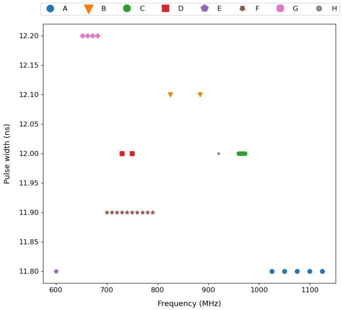

Frequency x Pulse Width.

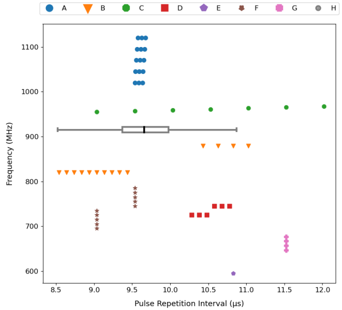

Pulse Repetition Interval x Frequency.

Figure: Emitters characteristics representation.

Pulse Repetition of Interval representation

- Discret process:

$$\mu_j = \sum_{n=1}^{N} \alpha_n \delta_{pri_n}, \quad (1)$$

with j the emitter index, N the number of PRIs on which the emitter transmits, α the proportion of the PRI, and δ, the Dirac mass (with $\sum \alpha_n = 1$).

- Random process:

$$P(x)_j = \frac{1}{\sigma_j \sqrt{2\pi}} \exp\left(-\frac{(x-\mu_j)^2}{2\sigma_j^2}\right), \quad (2)$$

with j the emitter index, μ of the PRI average value, and σ its standard deviation.

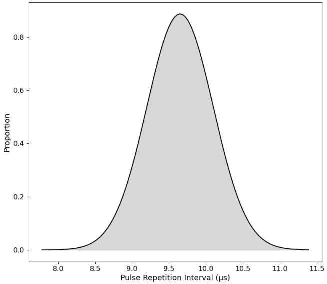

Figure: Random Pulse Repetition Interval.

Data acquisition

- Each train is composed of pulses, described by only 4 features:

$$pdw_i = \begin{pmatrix} f_1 & pw_1 & g_1 & toa_1 \\ f_2 & pw_2 & g_2 & toa_2 \\ \vdots & \vdots & \vdots & \vdots \\ f_m & pw_m & g_m & toa_m \end{pmatrix}, \qquad (3)$$

with i the train, m the pulses index, f the frequency, pw the pulse width, g the level and toa the time of arrival.

- Computation of the difference of time of arrival (DTOA): $dtoa_m = toa_m - toa_{m-1}$.

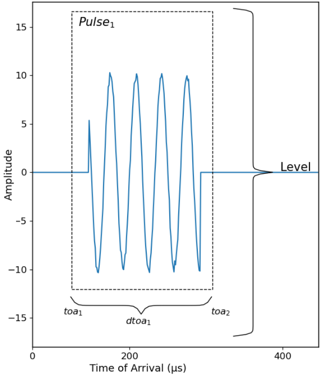

Figure: Example of a pulse from an intercepted signal.

Relation between the DTOA and the PRI

- Example of an Emitter with one PRI of $65ns$:

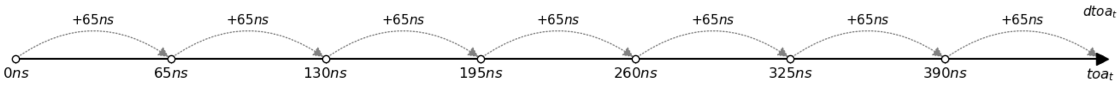

No noise, single emitter and all pulses intercepted $\Rightarrow PRI \equiv DTOA$

RADAR Signal example

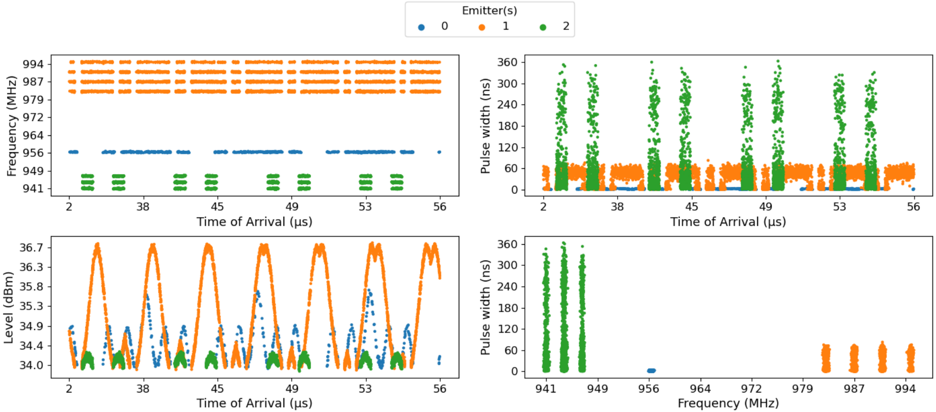

Figure: Example of a **simple** simulated signal grouping 8917 pulses from three emitters identified by color.

Application of the **RRP** on an intercepted signal

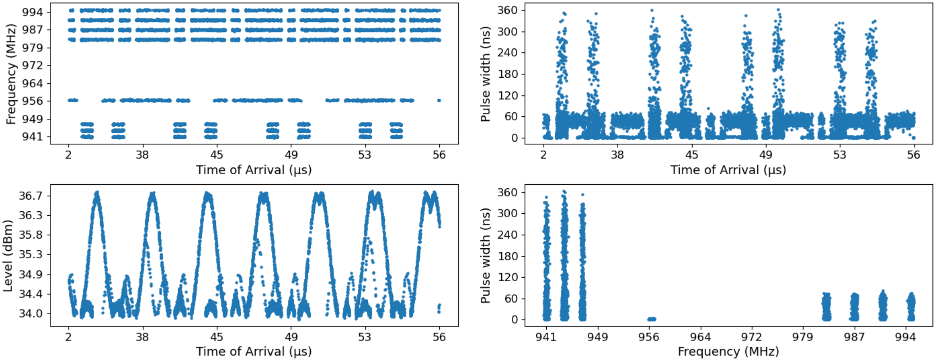

Content

Content

Hierarchical Agglomerative Clustering using Optimal Transport to deinterleave pulses - **HACOT**

2-step strategy

1. **Pulse separation**: Apply HDBSCAN [21] from frequency (F) and pulse width (PW).
2. **Cluster aggregation**: Apply a Hierarchical Agglomerative Clustering based on Optimal Transport distances [3, 22] from time of arrival (TOA) and level (G).

Step 1: Pulses separation with HDBSCAN

- Application of HDBSCAN on frequency (F) and pulse width (PW).
- Why HDBSCAN?
  - → Unsupervised algorithm,
  - → Search clusters of varying densities,
  - → Few parameters to optimize,
  - → May account for outliers (bring robustness to the proposed methodology).
- Over-estimation of the number of clusters:
  - → Some emitters don't transmit continuously,
  - → Each cluster must not contain the pulses of different emitters.

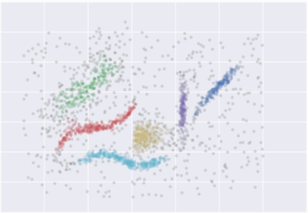

Credit: hdbscan.readthedocs.io.

HBSCAN outputs

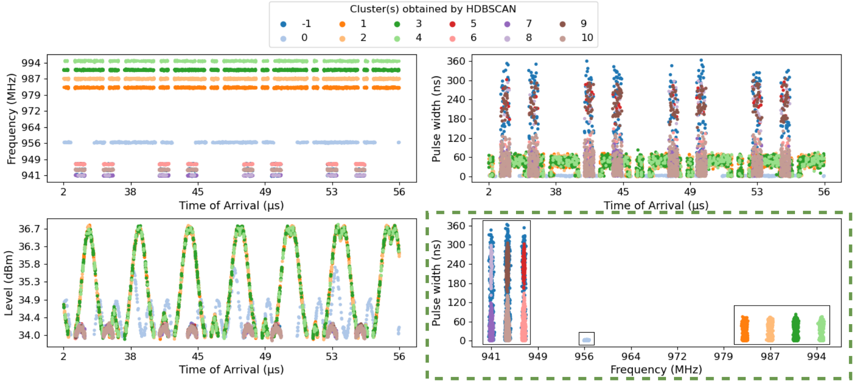

Clustering plane

Figure: Clustering results performed from frequency and pulse width. Each color represents clusters and a class of outliers (-1).

➜ How to group these clusters?

Step 2: Cluster aggregation with a Hierarchical Agglomerative Clustering based on Optimal Transport distances

Methodology

1. **Cluster representation** by a measure from time of arrival (TOA) and level (G),
2. **Distances computation** between clusters using **Optimal Transport distances**,
3. **Aggregation** of the two closest clusters,
4. **Updating distances**,
5. **Repeat** until a **single** cluster is obtained.

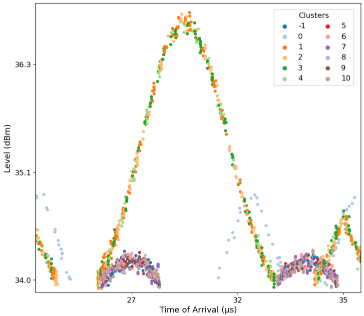

➜ How to define a distance between clusters using optimal transport distances?

Optimal Transport approach in 1 dimension

- **Intuition:** Compare clusters distributions to define a distance.
- Cluster 0 and Cluster 1 **belong** to the same emitter:
  - ✔ **Similar** distribution,
  - ✔ **Low** transport cost.
- Cluster 0 and Cluster 2 **don't belong** to the same emitter:
  - ✘ **Different** distribution,
  - ✘ **High** transport cost.

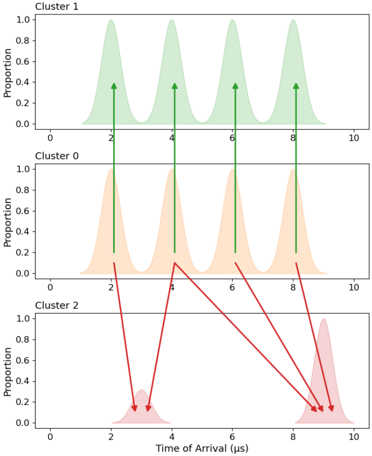

Optimal Transport (OT) explanation

- Consider transporting two discrete distributions $\mu_s = \sum_{n=1}^{N_s} \alpha_n \delta_{x_n}$ toward $\mu_t = \sum_{m=1}^{N_t} \beta_m \delta_{y_m}$.
- The total cost of a transport plan $\mathbf{P}$ is:

$$C(\mathbf{P}) = \sum_{n=1}^{N_s} \sum_{m=1}^{N_t} c(x_n, y_m)\mathbf{P}(x_n, y_m) = \langle \mathbf{C}, \mathbf{P} \rangle \,, \tag{4}$$

  with $C(\mathbf{P})$ the total cost, $c(x_n, y_m)$ the cost of transporting unit mass from x_n to y_m (transport cost) and $\mathbf{P}(x_n, y_m)$ the quantity of mass taken from x_n to y_m (transport plan).

- The optimal transport plan is a simple minimization problem:

$$\mathbf{P}^\star = \underset{\mathbf{P} \in (\mathbb{R}^+)^{N_s \times N_t}}{\operatorname{argmin}} \langle \mathbf{C}, \mathbf{P} \rangle \text{ such that } \mathbf{P}\mathbf{1}_{N_t} = \alpha \text{ and } \mathbf{P}^T \mathbf{1}_{N_s} = \beta. \tag{5}$$

Decisional model for pruning dendrogram based on unsupervised metrics and Optimal Transport distances

- Set aside Cluster 8,
- Decision model for pruning dendrogram based on:
  - → Gap Score to the optimal transport distances,
  - → Silhouette score [23],
  - → Calinski-Harabasz score [24],
  - → Davies-Bouldin score [25].

☛ **Majority rule** to get the optimal threshold.

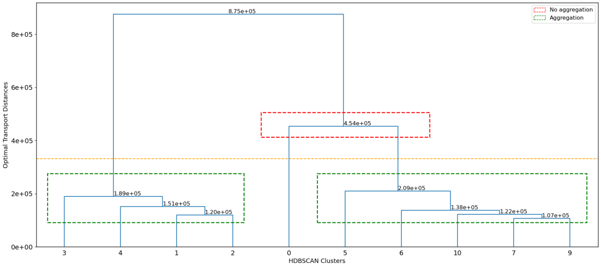

Figure: Cluster aggregations with Optimal Transport distances, the orange line highlights the optimal cut.

Hierarchical approach outputs

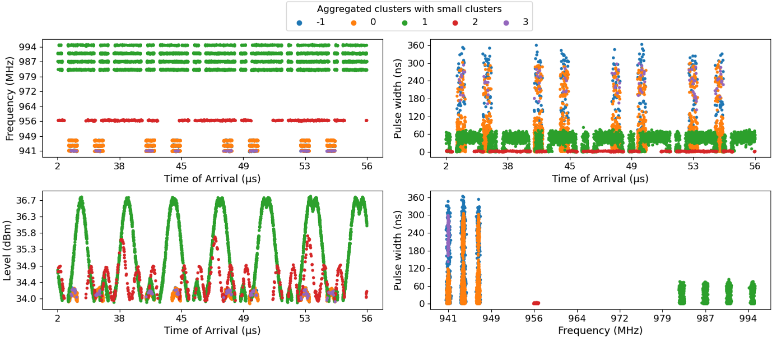

Figure: Aggregated clusters obtained according to the decision model and dendrogram resulting from the Hierarchical Agglomerative Clustering using Optimal Transport distances. Each color identifies an aggregated cluster with an outlier class (-1).

Dealing with excluded cluster

Application of a non-parametric method:

1. Estimation of the probability density of time of arrival of the extensive clusters i using a kernel density estimator with Gaussian kernel [26, 27, 28]:

$$\hat{f}_i(X) = \frac{1}{Nh} \sum_{i=1}^{N} K\left(\frac{x - x_i}{h}\right), \tag{6}$$

with N, the number of pulses, K, the kernel, h, and the smoothing parameter.

2. Association of an excluded cluster to an extensive cluster by maximum likelihood estimation:

$$L_i = \prod_{i=1}^{N} \hat{f}_i(t_n), \tag{7}$$

$$i^\star = \operatorname{argmax} L_i. \tag{8}$$

Final grouping

- Perfect grouping
- Statistics to evaluate the groupings:
  - ✔ Homogeneity [29] $= 1$
  - ✔ Completeness [29] $= 1$
  - ⚠ Unclassified rate $= 4.5\%$

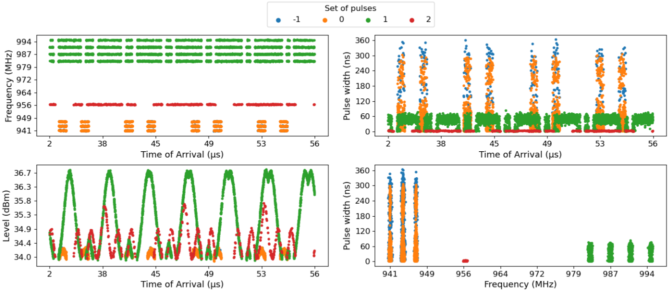

Figure: Final grouping identifying by a color with an outlier class (-1).

But sometimes...the reality is more complex...

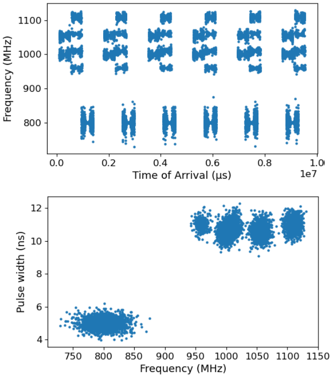

Intercepted signal.

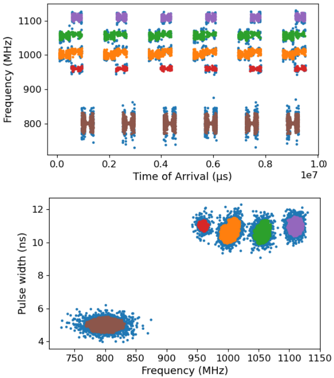

HDBSCAN outputs made in 2D.

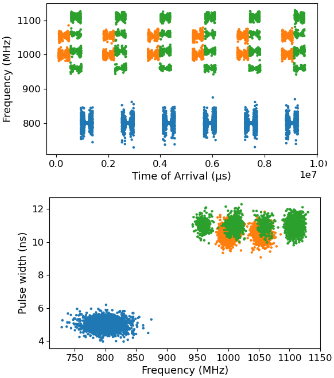

Ground labels.

Content

Improved Hierarchical Agglomerative Clustering using Optimal Transport to deinterleave pulses - **IHACOT**

3-step strategy

1. **Pulse separation**: Apply HDBSCAN from time of arrival (TOA), frequency (F), and pulse width (PW).
2. **Pre-clusters aggregation**: Apply a hierarchical agglomerative clustering from frequency (F) based on cluster averages pulse frequencies ($\overline{f_n}$) and width ($\overline{pw_n}$).
3. **Cluster aggregation**: Apply hierarchical agglomerative clustering based on optimal transport distances [3, 22] from time of arrival (TOA) and level (G).

Data description

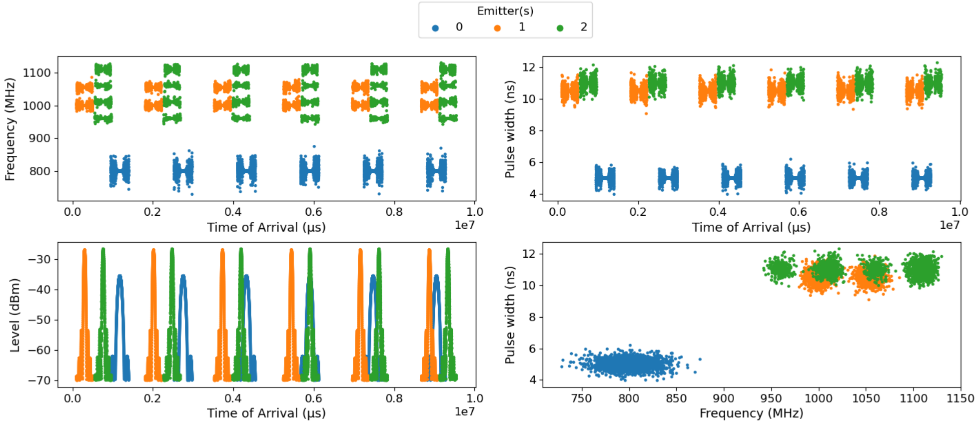

Figure: Example of a simulated signal gathering 22760 pulses of three emitters, represented by a color.

Step 1: Pulses separation with HDBSCAN

- Application of HDBSCAN on time of arrival, frequency, and pulse width:
  - → Better separability,
  - → Avoid pulses mixing,
  - → Temporal clusters.

➜ How to group simultaneously active clusters characterized by the same frequencies and pulse widths?

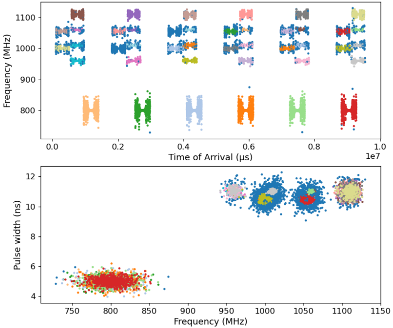

Figure: Clustering results performed in 3 dimensions. HDBSCAN detects 42 clusters with an outliers class (-1) identified by colors.

Step 2: Pre-clusters aggregation with a Hierarchical Agglomerative Clustering based on Euclidean distance

Methodology

1. **Cluster separation** by estimating cluster average pulse frequencies ($\overline{f_n}$) and width ($\overline{pw_n}$),
2. **Cluster aggregation** by applying a Hierarchical Agglomerative Clustering using Euclidean distances from frequency (F),
3. **Dendrogram pruning** according to a decisional model from time of arrival (TOA).

Step 2.1: Estimation of clusters averages frequencies and pulse widths

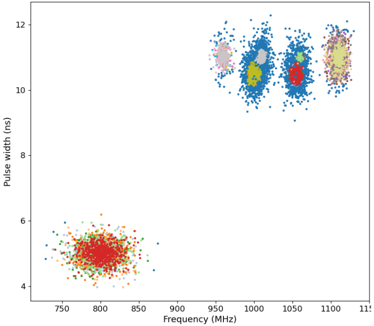

Clusters representation in the (f_n, pw_n) plane.

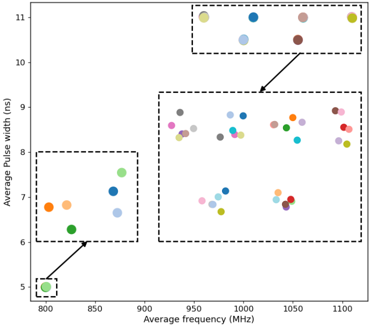

Cluster averages' representation in the (f_n, pw_n) plane.

Figure: HDBSCAN clustering results performed in 3 dimensions.
HDBSCAN detects 42 clusters with an outliers class identified by colors.

Step 2.2: Cluster aggregation with Hierarchical Agglomerative Clustering

- Apply a Hierarchical Agglomerative Clustering based on Euclidean distance from frequency,
- Set aside pulse width due to excessive estimation error,
- Previous decisional model is not suitable due to many clusters.

➜ How to stop aggregation?

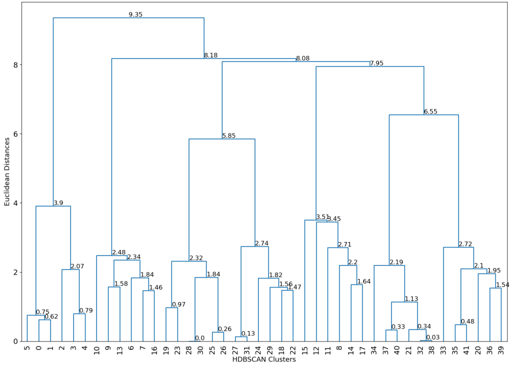

Figure: Dendrogram representing the aggregations at each iteration with the logarithm Euclidean distances values displayed.

Step 2.3: Improved decisional model for pruning the dendrogram based on statistical test

Methodology

I. **Selection of the first two aggregated clusters** according to the hierarchical structure,

II. **Computation of the Kolmogorov-Smirnov test** from time of arrival (TOA),

III. **Comparison of the p-value** with a **confidence threshold α**:

  if p-value $< \alpha$: do not consider all aggregation using these clusters,

  else select the next aggregation composed of the two aggregated clusters and repeat from (II).

IV. **Repeat** until all aggregations are evaluated.

➜ How to set the confidence threshold?

The Elbow Trick for fixing the confidence level

- Sorting *p*-values in ascending order,
- Identifying the **first** breakpoint,
- Confidence level: $\alpha_{ks} = 4.74 \times 10^{-4}$.

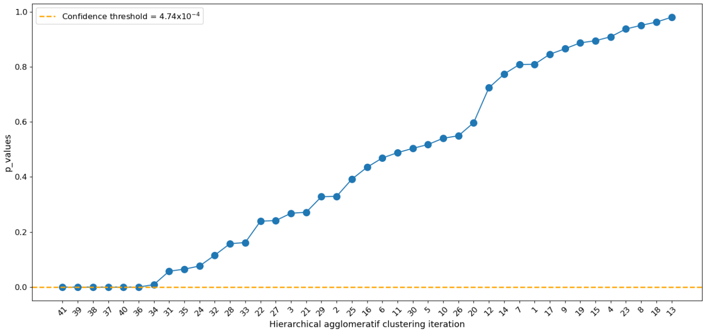

Figure: *p*-values sorted according to the Kolmogorov-Smirnov test, and the orange line highlights the estimated confidence level.

Elbow Tricks outputs

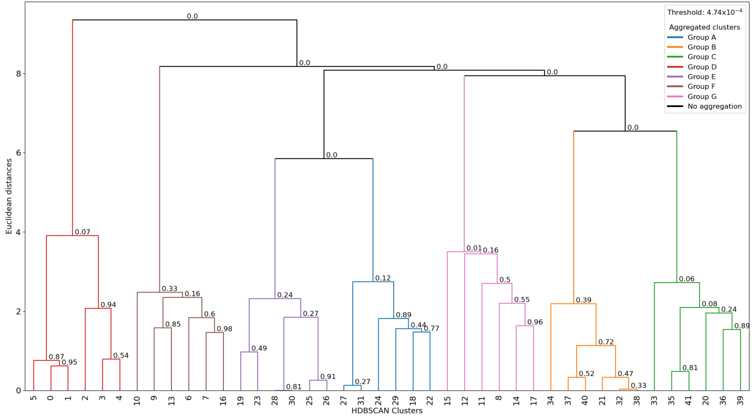

Figure: Hierarchical agglomerative clustering results according to the Kolmogorov-Smirnov test outputs. Each color identifies a cluster aggregate, and the Kolmogorov-Smirnov p-values are displayed.

Pre-clusters aggregation outputs

- Require another grouping phase,
- Application of the previous Hierarchical Agglomerative Clustering based on Optimal Transport distances [3, 22] from time of arrival (TOA) and level (G).

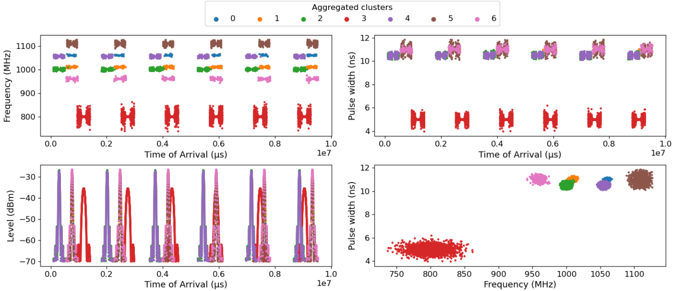

Figure: Aggregated clusters obtained following the Hierarchical Agglomerative Clustering using Euclidean distances pruning with Kolmogorov-smirnov test. Each color represents an aggregated cluster.

Step 3: Cluster aggregation with a Hierarchical Agglomerative Clustering based on Optimal Transport distance

- Satisfactory separation
- Statistics to evaluate the groupings:
  - ✔ Homogeneity [29] $= 1$
  - ✔ Completeness [29] $= 1$
  - ⚠ Unclassified rate $= 9\%$

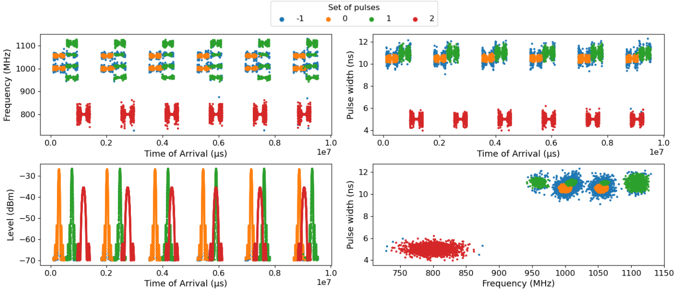

Figure: Final grouping after applied Hierarchical Agglomerative Clustering combined with Optimal Transport distances. Each color identified a set of pulses with an outliers class (-1).

Content

Requirements

- Deinterleaving set of pulses as an input:

Hypothesis: 1 set of pulses = 1 RADAR.

- Database with more than **60 classes** described by only three features:
  - Frequency (f_n),
  - Pulse width (pw_n),
  - Pulse Repetition of Interval (pri_n).

☛ **Identification up to the sub-mode.**

Content

Proximity analysis between emitters classes

⚠ Some emitters share similar characteristics and could be confused.

- **Intuition:** Compare emitters classes distributions using Optimal Transport distances.
  - ✔ Green: **High** transport cost,
    - → Emitters have **different** characteristics,
    - → **Low** risk of confusion.
  - ✘ Red: **Low** transport cost,
    - → Emitters share **close** characteristics,
    - → **Easy confusion**.

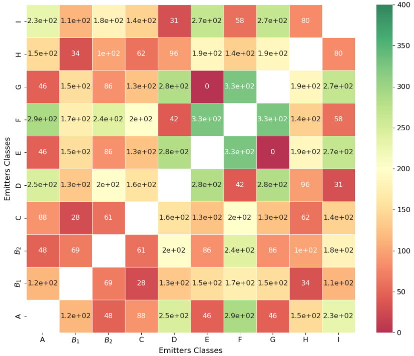

Figure: Cost matrix get from frequency and pulse width.

Optimal transport planes from frequency and pulse width

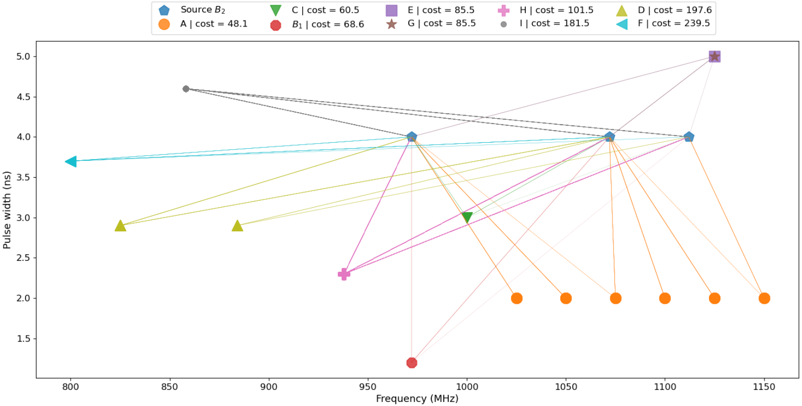

Figure: Optimal transport planes between emitter B_2 characteristics toward other emitters from Frequency and Pulse Width.

Content

IDdentification of emitters using Optimal Transport Distances - IDOT

3-step strategy

1. **Set of pulses representation**: Construction of a probability distribution based on the temporal emission pattern (DTOA), the frequency (F), and the pulse width (PW).
2. **Emitter class representation**: Construction of a discrete measure based on the temporal emission pattern (PRI_{mod}), the frequency (F), and the pulse width (PW).
3. **Identification of the emitter class**: Assignment of the closest class in the sense of optimal transport.

Step 1: Set of pulses representation

- Construction of a probability distribution from the deinterleaving set of pulses based on differentiated arrival time, frequency, and pulse width:

$$\nu = \frac{1}{M} \sum_{m=1}^{M} \delta_{dtoa_m, f_m, pw_m}, \tag{9}$$

with M, the number of pulses in the set and $dtoa_m = toa_m - toa_{m-1}$.

Step 2: Emitter class representation

✘ Signal can be noisy or poorly estimated:

$\Rightarrow$ Missing some pulses,

$\Rightarrow$ Distortion of the reconstruction of the PRI pattern from a set of pulses,

$\Rightarrow$ *pri* distribution of emitter from database **does not correspond** to the *dtoa* distribution of the set of pulses,

$\Rightarrow$ All research-based methods of PRI **inefficient**.

Missing pulses $\Rightarrow PRI \not\equiv DTOA$

Simple case: Emitter with one PRI

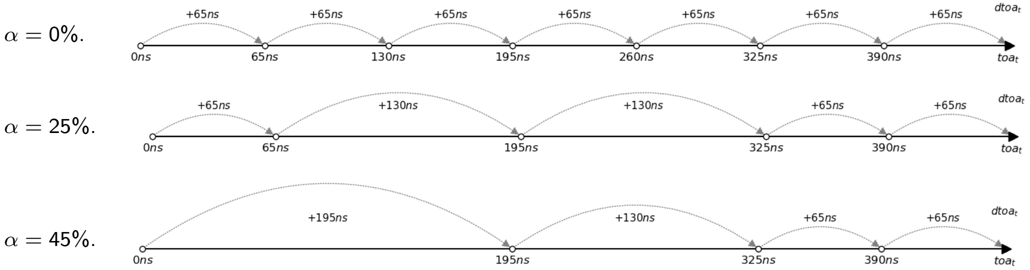

Figure: Example of the *dtoa* values according to different missing pulse rates α, of Emitter E.

⚠ Multiple *pri* distributions.

Pulse Repetition of Interval Modeling process according to the Missing Pulses Rate

- **Intuition**: Modeling the PRI values according to the missing pulse rate,
- Using the total probability formula,
- Consider N, the discrete random variable representing the number of missing pulses.

Methodology

1. **Missing pulses representation** according to a missing pulses rate $\mathbb{P}(N = n)$,
2. ***dtoa* distribution representation for a fixed number of missing pulses** $\mathbb{P}(dtoa = t|N = n)$,
3. **Representation of the *dtoa* distribution conditionally to the number of missing pulses**, $\mathbb{P}(dtoa = t)$.

Focus on the discrete process

1. Assuming that the losses are independent, a geometric distribution can represent them:

$$\mathbb{P}(N = n) = (1 - \alpha)\alpha^n, \tag{10}$$

2. Assuming that the values of *pri* have uniform probabilities of appearance the sum of successive *pri* starting with the k^{th} value of *pri*, one have:

$$t_{nk} = \sum_{m=k}^{k+n} pri_{m,mod[K]} \Rightarrow \mathbb{P}(dtoa = t | N = n) = \frac{1}{K}\sum_{k=0}^{K-1} \delta_{t_{nk}}. \tag{11}$$

3. from Equations (10), and (11):

$$\nu_\alpha = \frac{1}{K}\sum_{n=0}^{\infty}(1 - \alpha)\alpha^n \sum_{k=1}^{K} \delta_{t_{nk}}. \tag{12}$$

where α is the missing pulses rate, and K is the number of *pri* of the considering emitter.

☛ Generalizable to the continuous case by considering mixtures of Gaussians.

Application to Emitter E, C, and H

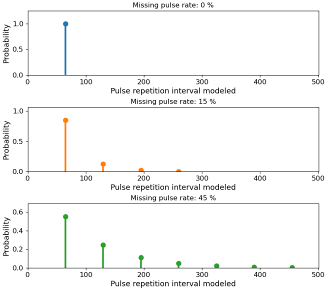

Emitter E with one PRI value.

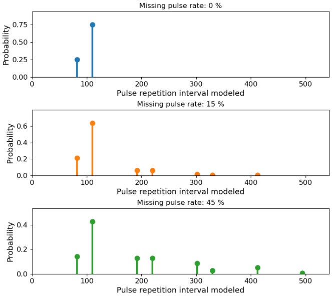

Emitter C with two PRI values.

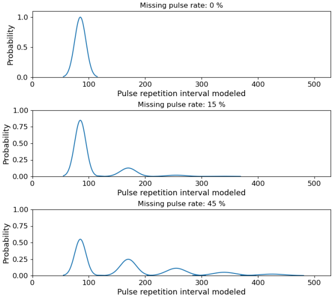

Emitter H with a random PRI.

Figure: Modelization of the *dtoa* distributions for different emitters according to different missing pulse rates.

Step 3: Identification Algorithm

- Identification of the emitter class by assigning the closest emitter in the optimal transport distance sense to each set of pulses:

$$j^{\star} = \underset{\mathbf{j} \in (1,\ldots,J)}{\operatorname{argmin}} \; d\left(\nu, \tau_j\right), \tag{13}$$

with J the number of emitters classes

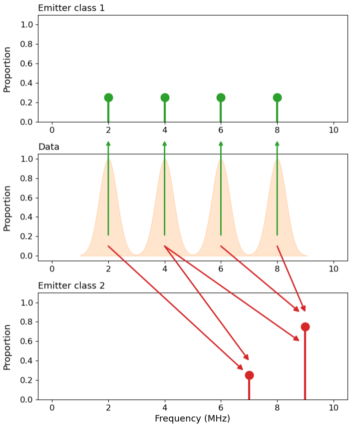

Identification output for Emitter C

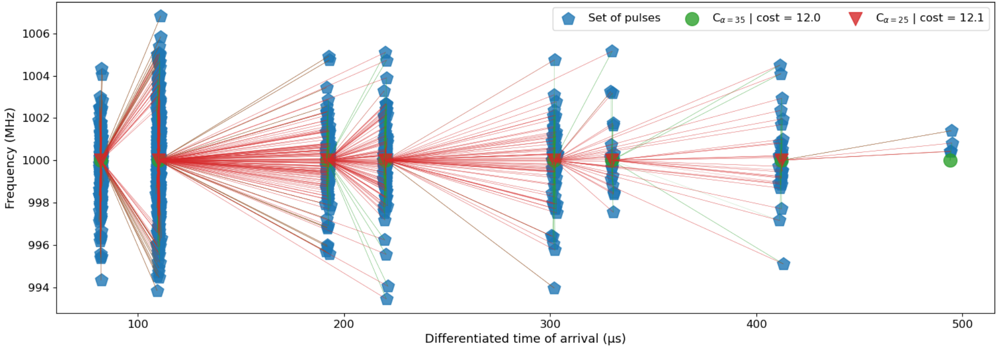

Figure: Identification outputs for Emitter C characterized by 2 PRI values (82*ns* and 110*ns*) with 35% of missing pulses. The plane overlaps the pulses and the characteristic points of the two first outputs identified by the algorithm.

Content

Content

Simulated signal

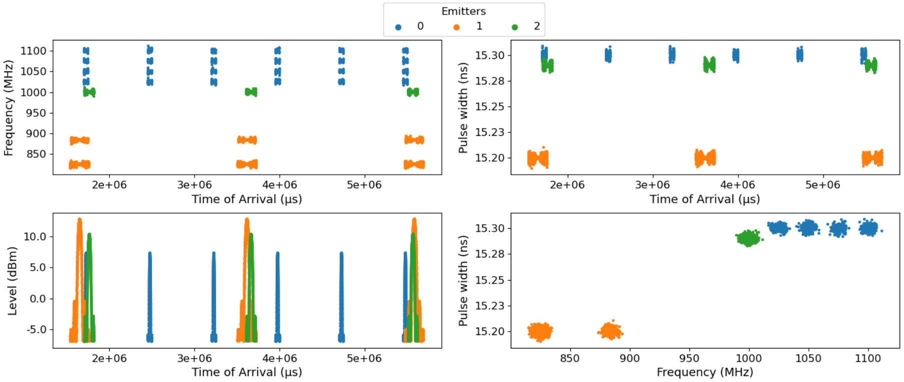

Figure: Simulated signal gathering 10044 pulses from 3 emitters, identified by a color.

Sensitivity to estimation errors

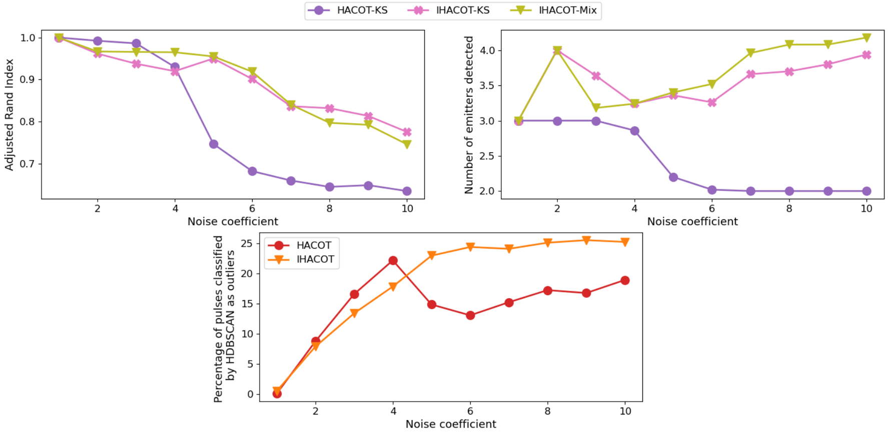

Figure: Performance of deinterleaving methods according to the noise added with ARI, number of emitters detected, and part of pulses classified by HDBSCAN as outliers. Each curve identifies a method.

Experimentation outputs

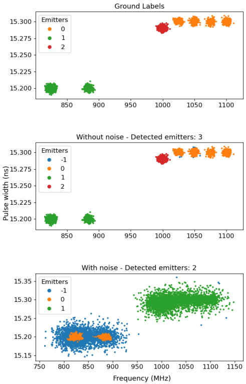

HACOT-KS.

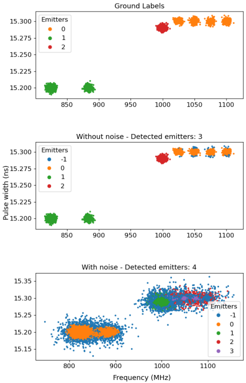

IHACOT-KS.

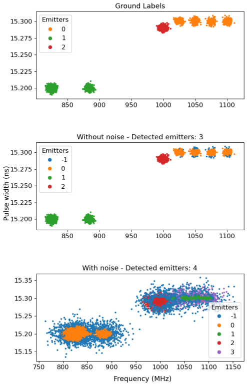

IHACOT-Mix.

Figure: Pulse's representation in the (f_n, pw_n) plane according to the deinterleaving results without noise and the baseline level is multiplying by 4.

Content

Emitters classes characteristics

Name	Frequency (MHz)	Pulse width (ns)	PRI (μs)
A	1025, 1050, 1075 1100, 1125, 1150	2	1520, 1540, 1560, 1580, 1600, 1620 1640, 1660, 1680, 1700, 1720, 1740 1760, 1780, 1800, 1820, 1840, 1860 1880, 1900, 1920, 1940, 1960, 1980
B	972	1.2	2000, 2200, 2400
C	972, 1072, 1112	4	2200
D	1000	4	1700, 2200
E	825, 884	2.9	1700, 1720, 1740, 1760, 1780, 1800, 1820 1840, 1860, 1880, 2080, 2120, 2160, 2200
F	800	3.7	1700, 1800, 1900, 2000, 2100, 2200, 2300, 2400
G	938	2.3	Min: 1700, Max: 1900

Table: Simulated emitters characteristics.

Proximity between emitters

⚠ Emitters with close characteristics:

- ✔ **High** transport cost: Different characteristics
- ✘ **Low** transport cost: Risk of confusion

⚠ Less clear-cut results,

⚠ Must pay attention to all classes.

Figure: Cost matrix get from pulse repetition of intervals, frequency, and pulse width.

Robustness against mixing pulses

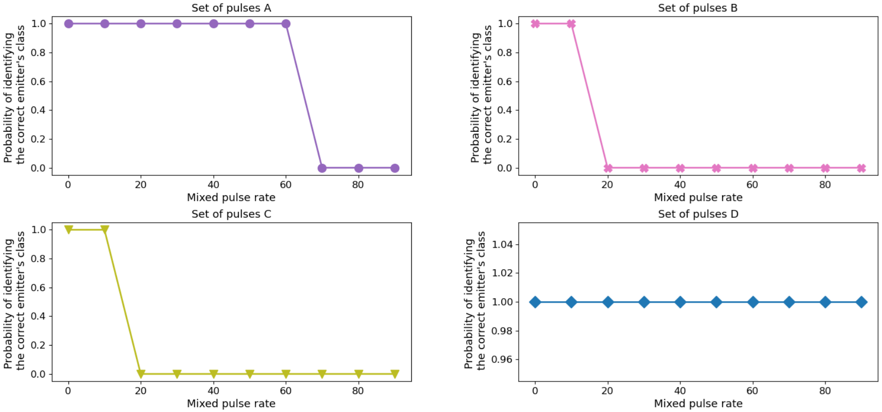

Figure: IDOT performance by analyzing the probability of identifying the correct emitter for each set of pulses according to several mixing pulse rates.

Experimentation outputs

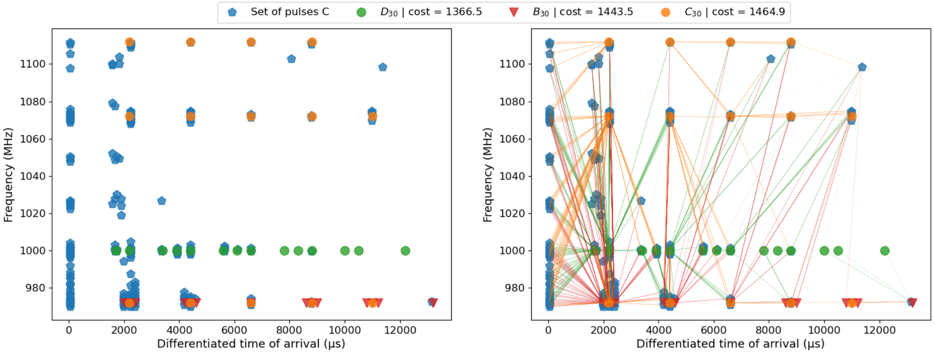

Figure: IDOT results for Set of pulses C characterized by a PRI (2200 ns) and 3 frequencies (972, 1072, 1112 MHz) with a mixing rate of 40% in the $(f_n, dtoa_n)$ plane.

Content

Conclusions

- Development of two **unsupervised** deinterleaving methods based on accessible and reliable features:
  - Works on moderately complicated cases with few data,
  - Avoid merging pulses belonging to different RADARs.
- Development of a new identification method based on PRI modeling:
  - **Insensitive** to missing pulses,
  - Methodology can handle a large number of classes to identify.
- Empirical results highlighting the robustness of the RADAR Recognition Process.

Perspectives

- **Deinterleaving RADAR pulses:**
  - Add temporarily available features and incorporate outliers in the process,
  - Handle cases where the RADAR clusters are not simultaneously active,
  - Analyze other breakpoints when setting the confidence threshold to stop dendrogram aggregations.
- **Identification of RADAR:**
  - Explore alternative methods to represent random PRI instead of Gaussian distribution,
  - Modeling the frequency according to different levels of outliers,
  - Add temporarily available features.
- Considering adverse countermeasures introducing disruptive signals and deploying the processes in real-time.

Scientific contributions (Mottier, Chardon, and Pascal)

Articles in peer-reviewed journals

- ✍ "Specific Emitter Identification based on Optimal Transport Distances and the Missing Pulses Rate Modelization for the Pulse Repetition of Intervals." - IEEE Aerospace and Electronic Systems Society 2024 (in writing).
- ✔ "Deinterleaving RADAR emitters with Optimal Transport Distances." - IEEE Aerospace and Electronic Systems Society 2024.

Conferences with proceedings

- ✔ "Désentrelacement et classification des émetteurs RADARs basés sur l'utilisation des distances de Transport Optimal." - CAID 2022.
- ✔ "Désentrelacement et classification de signaux RADAR basés sur des distances de transport optimal." - GRETSI 2022.
- ✔ "RADAR Emitter Classification with Optimal Transport Distances." - EUSIPCO 2022.
- ✔ "Deinterleaving and Clustering unknown RADAR pulses." - IEEE Radar Conference 2021.

Patents

- ✔ "Procédé d'identification d'un émetteur radar et système d'identification associé" - 2023
- ✔ "Procédé de désentrelacement d'impulsions RADAR" - 2023

Thank you for your attention!

CentraleSupélec
université PARIS-SACLAY
L2S Laboratoire Signaux & Systèmes
AVANTIX
MINISTÈRE DES ARMÉES
Liberté
Égalité
Fraternité
DGA

Annexes

Complex case: Emitter with two PRI values [1/2]

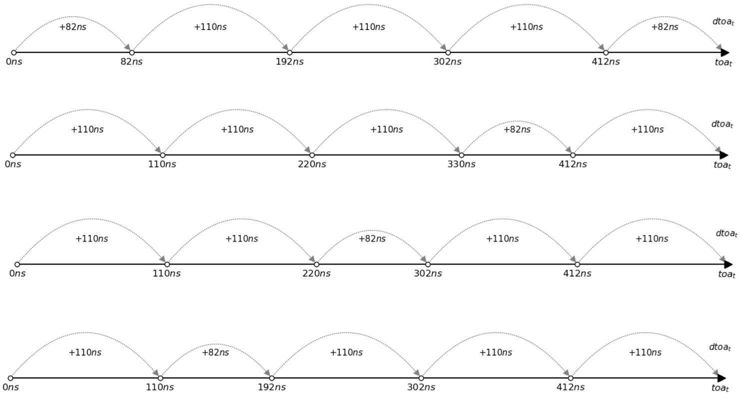

Figure: *dtoa* distribution when $\alpha = 0\%$ for a PRI pattern of $[82, 110, 110, 110]$.

Complex case: Emitter with two PRI values [2/2]

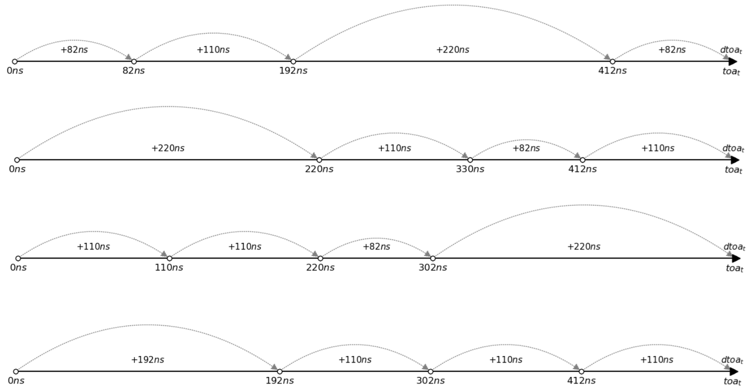

Figure: *dtoa* distribution when $\alpha = 25\%$ for a PRI pattern of $[82, 110, 110, 110]$.

Focus on the continuous process

1. Assuming that the losses are independent, a geometric distribution can represent them:

$$\mathbb{P}(N = n) = (1 - \alpha)\alpha^n, \tag{14}$$

2. The *pri* is represented by a Gaussian random variable J_m with mean pri_m and variance σ^2; assuming that the J_m are independent one have:

$$J_m \sim \mathcal{N}(pri_m, \sigma^2) \text{ and } T_{nk} = \sum_{m=k}^{k+n} J_m \text{ with } T_{nk} \sim \mathcal{N}(t_{nk}, (n+1)\sigma^2).. \tag{15}$$

3. from Equations (14), and (15):

$$p_\alpha(t) = \frac{1}{K} \sum_{n=0}^{\infty} (1 - \alpha)\alpha^n \sum_{k=1}^{K} p_{nk}(t), \tag{16}$$

where α is the missing pulses rate, and K is the number of *pri* of the considering emitter, p_{nk} is the density of the Gaussian variable T_{nk} and T_{nk} the law of the *dtoa*.

Content

Simulated signal

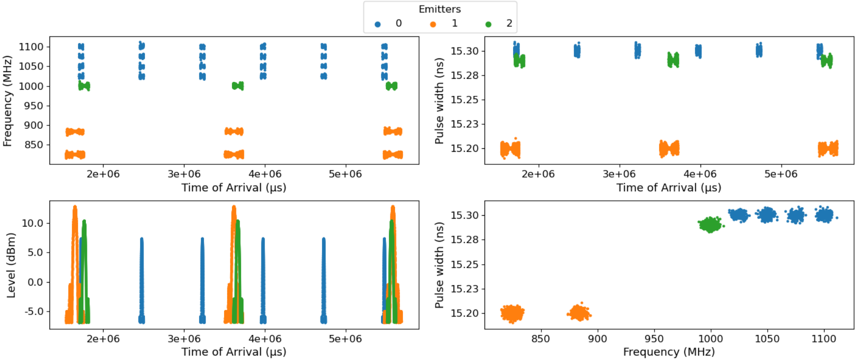

Figure: Simulated signal gathering 10044 pulses from 3 emitters, identified by a color.

Comparison with PRI-based methods

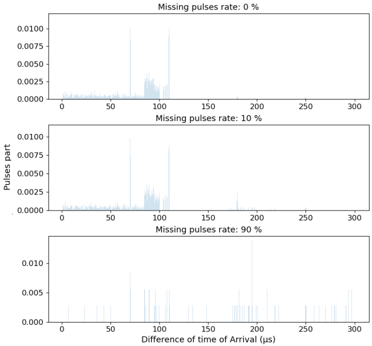

Mardia.

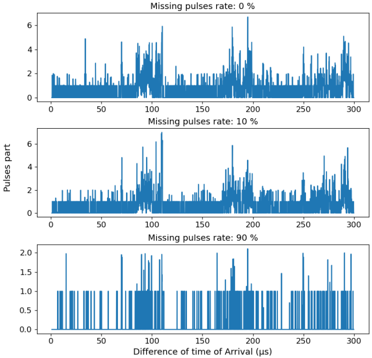

PRI Transform.

Figure: Outputs of the PRI-based methods to deinterleave the simulated signal according to different missing pulse rates.

Robustness to outliers

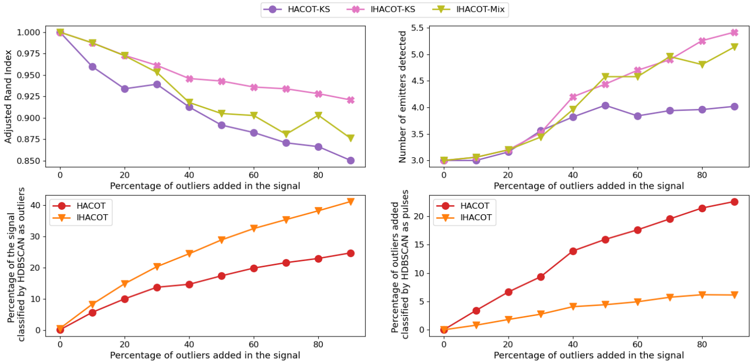

Figure: Performance of deinterleaving methods according to the outliers rate added with ARI, number of emitters detected, part of the pulses classified by HDBSCAN as outliers, and part of outliers added in the signal classified in the sets of pulses. Each curve identifies a method.

Experimentation outputs

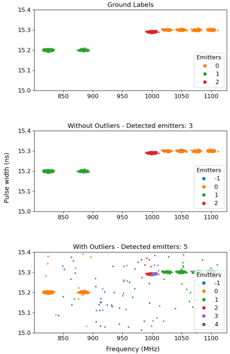

HACOT-KS.

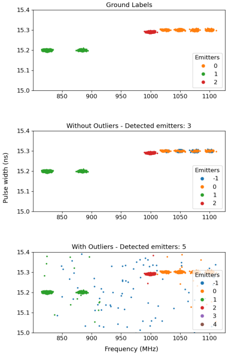

IHACOT-KS.

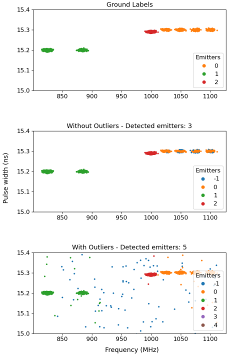

IHACOT-Mix.

Figure: Pulse's representation in the (f_n, pw_n) plane according to the deinterleaving results without outliers and when 90% of outliers is added.

Performance against missing pulses

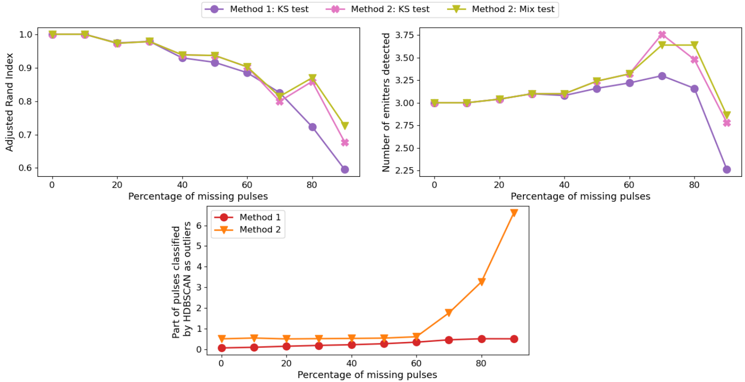

Figure: Performance of deinterleaving methods against missing pulses with ARI, number of emitters detected, and part of pulses classified by HDBSCAN as outliers. Each curve identifies a method.

Experimentation outputs

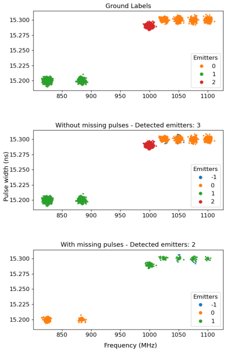

HACOT-KS.

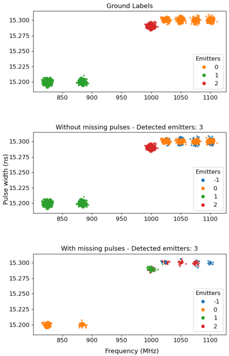

IHACOT-KS.

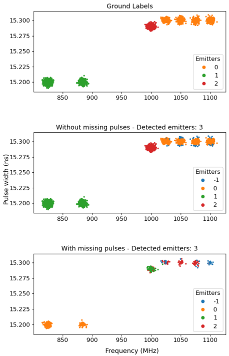

IHACOT-Mix.

Figure: Pulse's representation in the (f_n, pw_n) plane according to the deinterleaving results without missing pulses and when 90% of the pulses are missing.

Content

Robustness to outliers

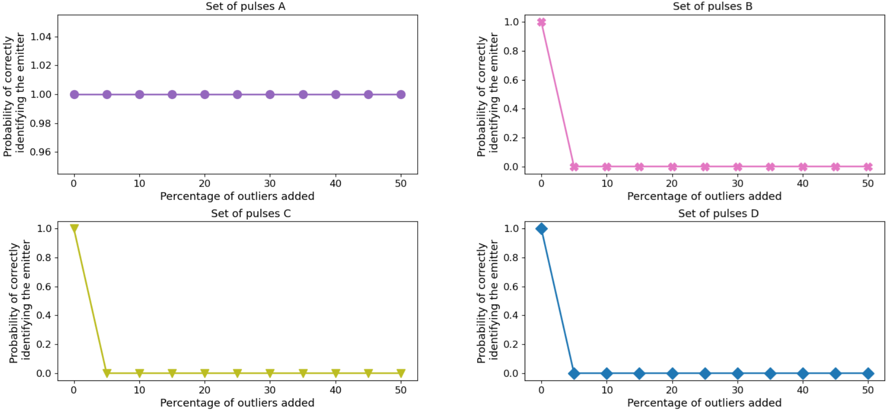

Figure: IDOT performance by analyzing the probability of identifying the correct emitter according to the outliers added for each set of pulses.

Experimentation outputs

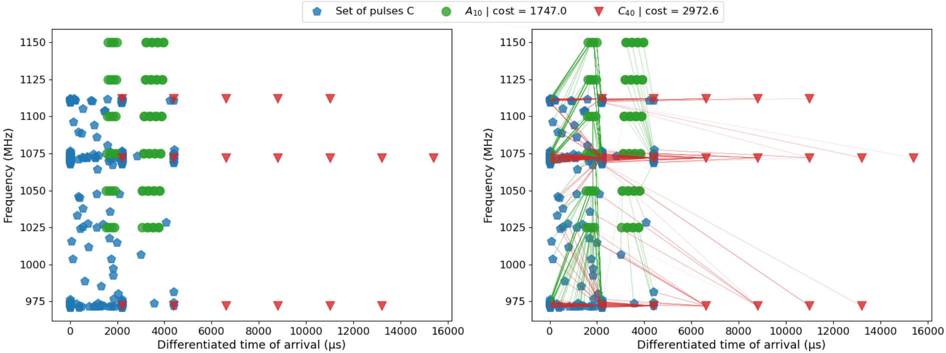

Figure: IDOT results for Set of pulses C with 40% of outliers added in the $(f_n, dtoa_n)$ plane.

Sensitivity to estimation errors

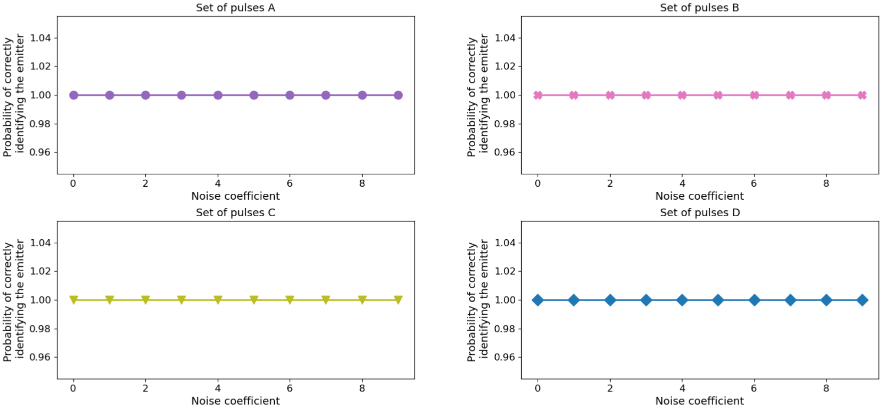

Figure: IDOT performance by analyzing the probability of identifying the correct emitter for each set of pulses when the variance level of the set of pulses is multiplied by a coefficient.

Experimentation outputs for Emitter C

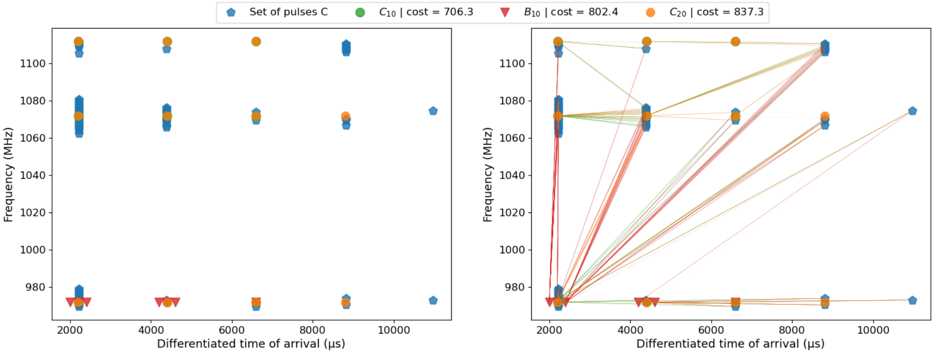

Figure: IDOT results for Set of pulses C when the baseline level is multiplying by 4.

Performance against missing pulse

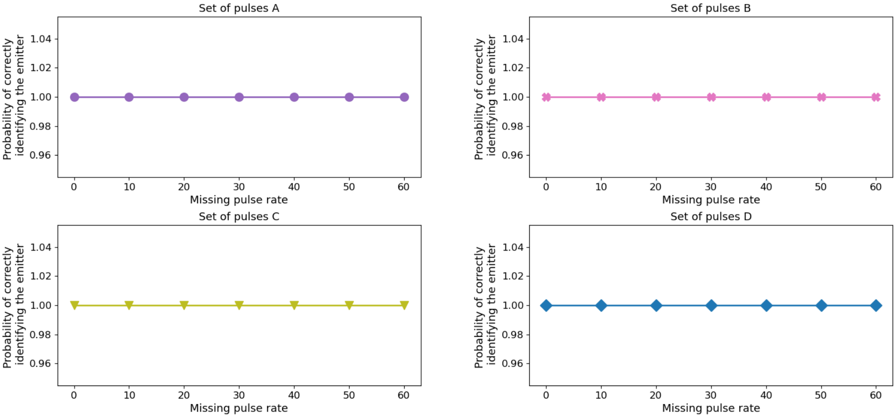

Figure: IDOT performance by analyzing the probability of identifying the correct emitter according to several missing pulse rate.

Experimentation outputs

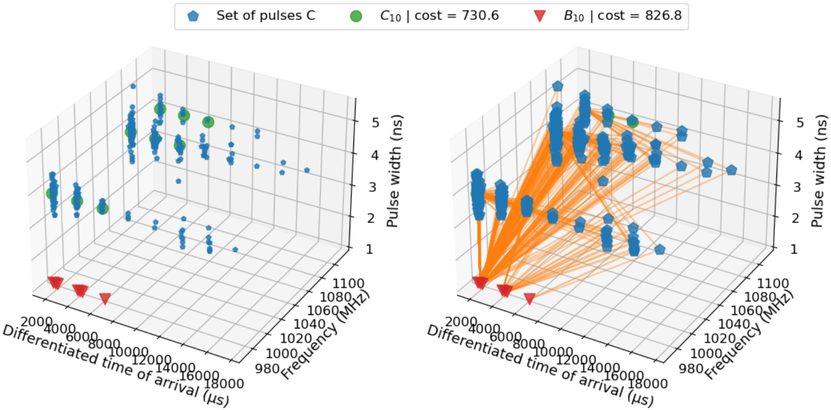

Figure: IDOT results plotted in 3 dimensions when 40% of pulses are missing for Set of pulses C.

Computational complexity

- **HACOT** [30]: $O(K^2(T^2\bar{R}^2 + \bar{C}^2 B))$

  with T the length of the signal, K the number of emitters, $\bar{R}$ the mean rate of pulses, $\bar{C}$ the mean number of clusters per emitter.

- **IHACOT**: $O(\bar{C}^3 K^3 T^3 S^3)$

  with $P = CTS$ the number of clusters identified by HDBSCAN where S is the average number of sweeps by second, and C is the number of pre-aggregation clusters.

- **IDOT** [31]: $O(B^2 J)$

  with J the number of classes, and B the number of bins representing the set of pulses.

References I

[1] Merrill I Skolnik. "Radar handbook". McGraw-Hill Education, 2008.

[2] Richard Wiley. "ELINT: The Interception and Analysis of Radar Signals". Artech, 2006.

[3] Cédric Villani. "Optimal transport: old and new". Vol. 338. Springer, 2009.

[4] Rémi Flamary, Nicolas Courty, Alexandre Gramfort, Mokhtar Z. Alaya, Aurélie Boisbunon, Stanislas Chambon, Laetitia Chapel, Adrien Corenflos, Kilian Fatras, Nemo Fournier, Léo Gautheron, Nathalie T.H. Gayraud, Hicham Janati, Alain Rakotomamonjy, Ievgen Redko, Antoine Rolet, Antony Schutz, Vivien Seguy, Danica J. Sutherland, Romain Tavenard, Alexander Tong, and Titouan Vayer. "POT: Python Optimal Transport". In: Journal of Machine Learning Research 22.78 (2021), pp. 1–8. URL: http://jmlr.org/papers/v22/20-451.html.

[5] Wilfrid Gangbo and Robert J McCann. "The geometry of optimal transportation". In: (1996).

[6] D. R. Wilkinson and A. W. Watson. "Use of metric techniques in ESM data processing". In: vol. 132. 4. July 1985, pp. 229–232.

[7] Vaughan Clarkson and Pinaki S Ray. "Parallel Processing for Differencing and Histogramming". Tech. rep. ELECTRONICS RESEARCH LAB ADELAIDE (AUSTRALIA), 1993.

[8] DJ Milojević and BM Popović. "Improved algorithm for the deinterleaving of radar pulses". In: IEE Proceedings F (Radar and Signal Processing). Vol. 139. 1. IET. 1992, pp. 98–104.

[9] HK Mardia. "New techniques for the deinterleaving of repetitive sequences". In: IEE Proceedings F (Radar and Signal Processing). Vol. 136. 4. IET. 1989, pp. 149–154.

[10] Xin Dong, Yan Liang, and Jie Wang. "Distributed Clustering Method Based on Spatial Information". In: IEEE Access (2022).

[11] Matthew Scherreik and Brian Rigling. "Online estimation of radar emitter cardinality via Bayesian nonparametric clustering". In: IEEE Transactions on Aerospace and Electronic Systems 57.6 (2021), pp. 3791–3800.

References II

[12] Shuyuan Yang, Xinyi Zhao, Huiling Liu, Chen Yang, Tongqing Peng, Rundong Li, and Feng Zhang. "Deep Contrastive Clustering for Signal Deinterleaving". In: IEEE Transactions on Aerospace and Electronic Systems (2023), pp. 1–11. DOI: 10.1109/TAES.2023.3322971.

[13] Mengtao Zhu, Shafei Wang, and Yunjie Li. "Model-Based Representation and Deinterleaving of Mixed Radar Pulse Sequences With Neural Machine Translation Network". In: IEEE Transactions on Aerospace and Electronic Systems 58.3 (2021), pp. 1733–1752.

[14] Zhang-Meng Liu. "Pulse deinterleaving for multifunction radars with hierarchical deep neural networks". In: IEEE Transactions on Aerospace and Electronic Systems 57.6 (2021), pp. 3585–3599.

[15] Mustafa Atahan Nuhoglu, Yasar Kemal Alp, Mehmet Ege Can Ulusoy, and Hakan Ali Cirpan. "Image Segmentation for Radar Signal Deinterleaving Using Deep Learning". In: IEEE Transactions on Aerospace and Electronic Systems 59.1 (2023), pp. 541–554. DOI: 10.1109/TAES.2022.3188225.

[16] A. Kawalec and R. Owczarek. "Radar emitter recognition using intrapulse data". In: 15th International Conference on Microwaves, Radar and Wireless Communications (IEEE Cat. No.04EX824). Vol. 2. 2004, 435–438 Vol.2. DOI: 10.1109/MIKON.2004.1357059.

[17] Jarmo Lunden and Visa Koivunen. "Automatic Radar Waveform Recognition". In: IEEE Journal of Selected Topics in Signal Processing 1.1 (2007), pp. 124–136. DOI: 10.1109/JSTSP.2007.897055.

[18] Zhang-Meng Liu and Philip S. Yu. "Classification, Denoising, and Deinterleaving of Pulse Streams With Recurrent Neural Networks". In: IEEE Transactions on Aerospace and Electronic Systems 55.4 (2019), pp. 1624–1639. DOI: 10.1109/TAES.2018.2874139.

[19] Zhe Geng, He Yan, Jindong Zhang, and Daiyin Zhu. "Deep-Learning for Radar: A Survey". In: IEEE Access 9 (2021), pp. 141800–141818. DOI: 10.1109/ACCESS.2021.3119561.

[20] Mustafa Atahan Nuhoglu, Yasar Kemal Alp, and Fatih Cagatay Akyon. "Deep Learning for Radar Signal Detection in Electronic Warfare Systems". In: 2020 IEEE Radar Conference (RadarConf20). 2020, pp. 1–6. DOI: 10.1109/RadarConf2043947.2020.9266381.

[21] Ricardo JGB Campello, Davoud Moulavi, and Jörg Sander. "Density-based clustering based on hierarchical density estimates". In: Pacific-Asia conference on knowledge discovery and data mining. Springer. 2013, pp. 160–172.

References III

[22] Nicolas Bonneel, Michiel Van De Panne, Sylvain Paris, and Wolfgang Heidrich. "Displacement interpolation using Lagrangian mass transport". In: Proceedings of the 2011 SIGGRAPH Asia conference. 2011, pp. 1–12.

[23] Peter J Rousseeuw. "Silhouettes: a graphical aid to the interpretation and validation of cluster analysis". In: Journal of computational and applied mathematics 20 (1987), pp. 53–65.

[24] David L Davies and Donald W Bouldin. "A cluster separation measure". In: IEEE transactions on pattern analysis and machine intelligence 2 (1979), pp. 224–227.

[25] Tadeusz Caliński and Jerzy Harabasz. "A dendrite method for cluster analysis". In: Communications in Statistics-theory and Methods 3.1 (1974), pp. 1–27.

[26] Murray Rosenblatt. "Remarks on some nonparametric estimates of a density function". In: The annals of mathematical statistics (1956), pp. 832–837.

[27] Emanuel Parzen. "On estimation of a probability density function and mode". In: The annals of mathematical statistics 33.3 (1962), pp. 1065–1076.

[28] David W Scott, Richard A Tapia, and James R Thompson. "Nonparametric probability density estimation by discrete maximum penalized-likelihood criteria". In: The annals of statistics (1980), pp. 820–832.

[29] Andrew Rosenberg and Julia Hirschberg. "V-measure: A conditional entropy-based external cluster evaluation measure". In: Proceedings of the 2007 joint conference on empirical methods in natural language processing and computational natural language learning (EMNLP-CoNLL). 2007, pp. 410–420.

[30] Ricardo J. G. B. Campello, Davoud Moulavi, Arthur Zimek, and Jörg Sander. "Hierarchical Density Estimates for Data Clustering, Visualization, and Outlier Detection". In: ACM Trans. Knowl. Discov. Data 10.1 (July 2015). ISSN: 1556-4681. DOI: 10.1145/2733381.

[31] Pavel Dvurechensky, Alexander Gasnikov, and Alexey Kroshnin. "Computational optimal transport: Complexity by accelerated gradient descent is better than by Sinkhorn's algorithm". In: International conference on machine learning. PMLR. 2018, pp. 1367–1376.

Thank you!

CentraleSupélec

université PARIS-SACLAY

L2S Laboratoire Signaux & Systèmes

AVANTIX

MINISTÈRE DES ARMÉES
Liberté
Égalité
Fraternité

DGA

Still 5 minutes to go ...

Fight against gender-based and sexual violence

En avant toute(s): the association fights for gender equality and against sexism and sexual violence. It prevents violence, supports victims via a dedicated chat, and raises awareness among young people about school equality. Its objective: a caring, egalitarian society without discrimination or violence. [website]

Fondation des femmes: the Women's Foundation is the reference structure in France for the freedom and rights of women and against the violence of which they are victims. Supported by donations, this organization offers financial, legal, and material assistance to impact community initiatives across the country. [website]

Çapèse: it aims to promote gender equity within the CentraleSupélec campus. [website]

Fight against PhD students' harassment/discrimination

- **No association** specializing in the fight against discrimination and harassment of doctoral students...
- Some contacts:
  - Your PhD student representatives...
  - **CentraleSupélec**: work psychologist, official report ... [resources]
  - **Paris-Saclay University**: official report [ressources]
  - **JuriSup**: a professional network of legal affairs managers in higher education and research [ressources]
  - **Legal support**

Manon Mottier

www.manonmottier.com

manon-mottier

manon-mottier

0000-0003-4769-6159

CentraleSupélec

université PARIS-SACLAY

L2S Laboratoire Signaux & Systèmes

AVANTIX

MINISTÈRE DES ARMÉES
Liberté
Égalité
Fraternité

DGA